Journal of Theoretical Biology 337 (2013) 174–180

Contents lists available at ScienceDirect

Journal of Theoretical Biology

journal homepage: www.elsevier.com/locate/yjtbi

Modeling sphingomyelin synthase 1 driven reaction at the Golgi apparatus can explain data by inclusion of a positive feedback mechanism

Caterina Thomaseth [a,1], Patrick Weber [a,*,1], Thomas Hamm [a], Kenji Kashima [b], Nicole Radde [a]

[a] Institute for Systems Theory and Automatic Control, University of Stuttgart, Pfaffenwaldring 9, 70569 Stuttgart, Germany
[b] Graduate School of Engineering Science, Department of Systems Innovation, Osaka University, 1-3, Machikaneyama, Tokyonaka, Osaka 560-8531, Japan

HIGHLIGHTS

- Two models describing sphingomyeline synthesis reaction data are presented.
- A feedback model and a feedback free model is analyzed.
- Positive feedback from educts to products is sufficient to describe the data.
- Our theoretical investigations reject models without this feedback.
- The successor model motivates further investigations of the feedback.

ARTICLE INFO

Article history:
Received 21 November 2012
Received in revised form
19 August 2013
Accepted 21 August 2013
Available online 31 August 2013

Keywords:
Feedback control
Sphingomyelin synthase 1
Sphingomyelin synthesis

ABSTRACT

Here we present a minimal mathematical model for the sphingomyelin synthase 1 (SMS1) driven conversion of ceramide to sphingomyelin based on chemical reaction kinetics. We demonstrate via mathematical analysis that this model is not able to qualitatively reproduce experimental measurements on lipid compositions after altering SMS1 activity. We prove that a positive feedback mechanism from the products to the reactants of the reaction is one possible model extension to explain these specific experimental data. The proposed mechanism in fact exists *in vivo* via protein kinase D and the ceramide transfer protein CERT. The model is further evaluated by additional observations from the literature.

1. Introduction

Sphingomyelin synthase (SMS) is a class of enzymes that produce sphingomyelin (SM) by transferring a phosphocholine moiety from phosphatidylcholine (PC) on to ceramide, whereby diacylglycerol (DAG) is generated as a byproduct (Huitema et al., 2004). SMS consists of the two isoforms SMS1 and SMS2, which are mainly located at the Golgi apparatus and the plasma membrane, respectively (Huitema et al., 2004). The sphingolipids and glycerolipids in this reaction are involved in different cellular processes. Ceramide acts as a pro-apoptotic factor, while DAG is a mitogenic factor that is involved in cell proliferation and cell growth. SM is an abundant sphingolipid species, which has a high affinity for cholesterol and facilitates the formation of lipid rafts in the plasma membrane, which are known to have an effect on multiple signaling pathways. Thus, it is expected that, via regulation of levels of these lipids, SMS has the potential to regulate various cellular processes. In fact, a series of publications shows that SMS has multiple roles in cellular functioning such as proliferation, cell growth and survival (Tafesse et al., 2007), secretion (Sarri et al., 2011; Subathra et al., 2011) or apoptosis (Ding et al., 2008): Tafesse et al. (2007) used RNA inference to specifically deplete SMS from human cervical carcinoma HeLa cells and analyzed the effect on the Golgi- and plasma membrane-associated SMS activities, SM synthesis, overall lipid composition,

Abbreviation: Cer, ceramide; CHO Cells, Chinese hamster ovary cells; DAG, diacylglycerol; ER, endoplasmic Reticulum; IFT, implicit function theorem; PC, phosphatidylcholine; PH Domain, pleckstrin homology domain; PI, phosphatidylinositol; PI4P, phosphatidylinositol(4)-Phosphat; PI4KIIIβ, phosphatidylinositol-4-Kinase IIIβ; PKD, protein kinase D; SM, sphingomyelin; SMS, sphingomyelin synthase; TGN, trans-Golgi network

* Corresponding author. Tel.: +49 711 685 67754.
E-mail addresses: caterina.thomaseth@ist.uni-stuttgart.de (C. Thomaseth), patrick.weber@ist.uni-stuttgart.de (P. Weber).

[1] Authors contributed equally.

0022-5193
http://dx.doi.org/10.1016/j.jtbi.2013.08.022

and finally cell growth. According to their observations, the treatment of HeLa cells with SMS1 siRNA for 7 days lead to a 80% reduction of SMS activity, which resulted in a reduction of SM to about 80% of the control, while ceramide increased by a factor of 1.8. No significant changes were detected in PC and DAG levels. Villani et al. (2008) investigated the effect of SMS depletion and expression on DAG and showed that, while the total cellular DAG level was not significantly affected in dependence of SMS levels, SMS was able to manipulate subcellular pools of DAG. Of particular interest is the SMS1-mediated regulation of the DAG pool at the Golgi apparatus, which results in a reduction of localization of the DAG-binding protein PKD to the Golgi (Villani et al., 2008). To our knowledge, this is the first paper that hypothesizes a regulating role of SMS1 for secretion. This hypothesis was further investigated by Subathra et al. (2011), who addressed the role of SMSs in vesicular trafficking from the Golgi to the plasma membrane. They demonstrated in HeLa cells that inhibition of both SMS isoforms changes the Golgi morphology similar to inhibition of PKD, and that protein transport as well as secretion of an endogenous cargo like insulin were reduced. Recent work of Sarri et al. (2011) follows a similar line. Instead of modulating SMS activity they alter PC synthesis in CHO cells to evaluate the changes in DAG levels and its effect in membrane trafficking at the Golgi and observed a decrease in protein transport efficiency in response to DAG reduction. For a further summary of recent and past SMS related findings we refer to the review (Holthuis and Luberto, 2010).

Summarizing, these studies clearly demonstrate that SMS has an important impact on multiple cellular functions. In particular, modulation of SMS1, which localizes exclusively to the Golgi complex (Huitema et al., 2004; Tafesse et al., 2007), influences secretory transport via regulation of local lipid pools and their downstream effects on PKD (Subathra et al., 2011).

In this study we aim to build a mathematical model for the SMS1 driven conversion of ceramide to SM involving the two substrates ceramide and PC and the byproduct DAG and to explain the system's response to external manipulations on SMS1. We investigate whether a simple model, situated at the TGN, that only considers the direct reaction partners, is sufficient to reliably predict changes in cellular lipid pools in response to manipulations of SMS1 activity. This is done by using chemical reaction kinetics to describe the lipid concentrations as a function of SMS1 activity. Data are provided in Ding et al. (2008), where the effect of SMS knockdown and overexpression on SM, DAG, ceramide and PC and subsequent effects on apoptosis were studied in CHO and macrophage cells, respectively. Using mathematical analysis, we demonstrate that a model that only considers the reversible conversion reaction is not able to reproduce the observations qualitatively. However, by extending the model by a positive feedback loop between DAG and ceramide, based on biological knowledge on possible feedback mechanisms in the system including interactions between CERT and PKD, we show that the revised model can reproduce the data.

2. Model and data

2.1. Mathematical model

We consider the following chemical reaction, in which SMS1 uses ceramide and PC as substrates to produce SM and DAG:

$$\mathrm{Cer}+\mathrm{PC}\underset{\mathrm{SMS1}}{\overset{\mathrm{SMS1}}{\rightleftharpoons}}\mathrm{SM}+\mathrm{DAG} \tag{1}$$

Since this is known to be a reversible reaction, and SMS1 can in principle drive both directions (Huitema et al., 2004), we model it as such.

Describing this reaction using mass action (or any other kind of) kinetics in dependence of the input SMS1, lipid concentrations reach a steady state and the net flux is zero. The respective *in vivo* reaction is, however, a dynamic equilibrium with a rightward flow, since ceramide is continuously transported to the Golgi apparatus via CERT, and SM is transported away from the Golgi to the plasma membrane. Thus, concentrations reach a dynamic steady state, in which the system has in- and outflows, and the net flux of the reversible reaction does not disappear. To take this into account, we describe the system in the following way:

$\varnothing \overset{C_{in}}{\rightarrow} \mathrm{Cer}$	Influx of ceramide at the Golgi
$\mathrm{Cer} \overset{d_1}{\rightarrow} \varnothing$	Degradation of ceramide
$\mathrm{PC} = \mathrm{const}$	PC constant
$\mathrm{Cer}+\mathrm{PC}\underset{\mathrm{SMS1}}{\overset{\mathrm{SMS1}}{\rightleftharpoons}}\mathrm{SM}+\mathrm{DAG}$	SMS1 driven reversible reaction
$\mathrm{DAG} \overset{d_2}{\rightarrow} \varnothing$	Degradation of DAG
$\mathrm{SM} \overset{d_3}{\rightarrow} \varnothing$	Degradation and removal of SM

Here we have an influx of ceramide that describes CERT-mediated transport of ceramide from the endoplasmic reticulum (ER), where it is produced, to the Golgi apparatus. Furthermore, PC is assumed to be constant according to experimental data which indicate that PC does not change significantly when SMS1 is manipulated (Tafesse et al., 2007; Ding et al., 2008). This assumption can be interpreted as a dominant regulation of PC by other pathways, which balance the effect of SMS1, or by a large overall pool of PC, which is not affected by changes of small fractions. In fact, it is known that PC is present in the TGN membrane in high concentrations (van Meer et al., 2008), such that this is a reasonable assumption. Furthermore, ceramide, DAG and SM are subject to degradation and/or outflux, which are described by simple linear kinetics. In case of SM this term mainly describes the transport away from the TGN to the PM.

We want to compare two model versions that differ in their model boundaries, as depicted in Fig. 1A: Model 1 with tighter boundaries assumes a constant influx of ceramide, while this influx depends on DAG in the second model, which involves a biologically motivated feedback regulation from DAG to ceramide via the proteins PKD and PI4KIII β. Fig. 1B shows a simplified sketch of this indirect regulation scheme: DAG binds PKD and thereby recruits it to the TGN, where it is activated by the protein kinase PKC η via phosphorylation (Bard and Malhotra, 2006) and required for proper fission of transport vesicles. There are three PKD isoforms known, while particularly PKD1 and PKD2 are recruited to the trans-Golgi network (TGN) via their cysteine-rich Zn finger domain (CYS2) (Pusapati et al., 2010). The feedback regulation involves the ceramide transfer protein CERT, which mediates ceramide transport from the ER to the TGN membrane in a non-vesicular manner (Hanada et al., 2003; Kudo et al., 2008). Active PKD at the TGN has been shown to have a dual effect on CERT: on the one hand, it directly phosphorylates the SR motif of CERT thereby inhibiting the binding of CERT to PI4P at TGN membranes (Hausser et al., 2005). On the other hand, via activation of the kinase PI4KIII β (Fugmann et al., 2007), it triggers phosphorylation of the membrane lipid phosphatidylinositol (PI), whereby phosphatidylinositol(4)-phosphate (PI4P) is generated. The ceramide transfer protein CERT binds to PI4P via its pleckstrin homology (PH) domain, which enables binding of ceramide to the TGN membrane.

To integrate this regulation into the model, we assume that the velocity C_{in} of ceramide transport depends on the DAG level, $C_{in} = C_{in}(\mathrm{DAG})$. This is a very simplified description of the indirect influence of DAG on the ceramide level at the TGN, which

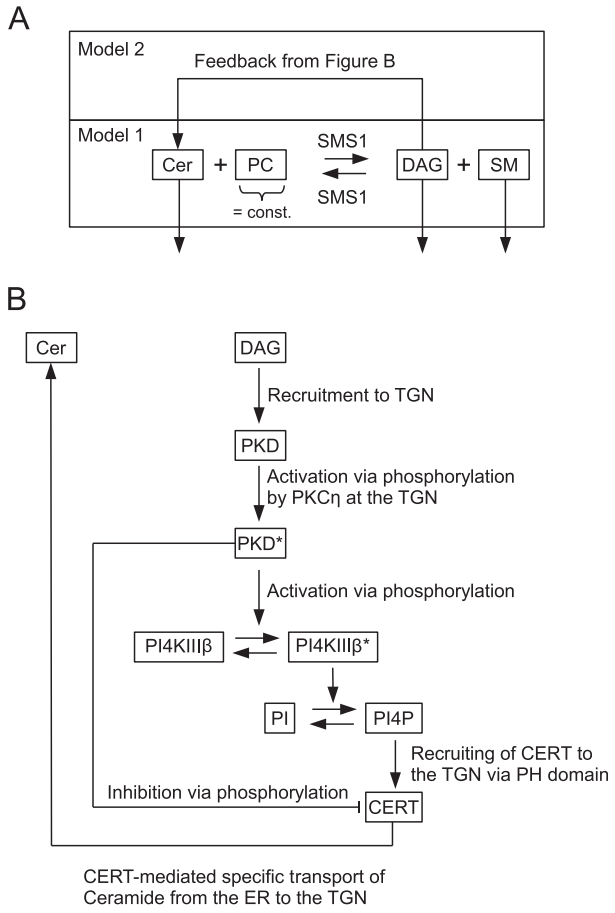

Fig. 1. (A) Illustration of model boundaries of models 1 and 2: Model 1 considers only the four lipids that take part in the SMS1 driven two substrate reaction, while model 2 includes a feedback from DAG to ceramide via PKD and CERT and (B) feedback regulation from DAG to ceramide at the TGN: DAG recruits PKD to the TGN, where it is activated via phosphorylation. Active PKD triggers the phosphorylation and thereby activation of the kinase PI4KIII β, with subsequent production of PI4P from PI. The ceramide transfer protein, which specifically recognizes ceramide via it's START domain and transports it from the ER to the TGN, binds via it's PH domain to PI4P at the TGN. This enables release of ceramide to the TGN, where it can be converted to SM.

summarizes all molecular interaction steps into one effective direct regulation.

Our system of ordinary differential equations reads

$$\begin{aligned}\dot{x}_1 &= C_{in} - d_1 x_1 - v(u, \mathbf{x}, [\mathrm{PC}]) \quad \text{Ceramide}\\ \dot{x}_2 &= -d_2 x_2 + v(u, \mathbf{x}, [\mathrm{PC}]) \quad \text{DAG}\\ \dot{x}_3 &= -d_3 x_3 + v(u, \mathbf{x}, [\mathrm{PC}]) \quad \text{SM}\end{aligned} \tag{2}$$

with

$$C_{in} = \begin{cases} \text{const.} & \text{for model 1 without feedback} \\ C_{in}(x_2) & \text{for model 2 with feedback} \end{cases} \tag{3}$$

and $\mathbf{x} = (x_1, x_2, x_3) =$ ([Cer],[DAG],[SM]). The input $u =$ [SMS1] describes changes in the activity of SMS1, and has a value of 1 for the control case. Parameters d_1, d_2 and d_3 describe the degradation rate constants. For the moment we assume v to be any reversible enzyme kinetics, e.g. Michaelis Menten or Hill type kinetics. We do not have to specify this further here, since our main results hold for the general case.

2.2. Interpretation of experimental data

To analyze the validity of the proposed model versions, i.e. the ability to reproduce real experimental findings, we used two

Table 1
Lipid concentrations and respective standard deviations in CHO cells overexpressing SMS1, which resulted in a 2.2-fold increase in cellular SMS1 activity. Values according to Table 1 in Ding et al. (2008) and normalized to the levels in the control experiments. Values labeled with an asterisk were marked as statistically significant changes compared to the control in the original publication.

Type of experiment	[Cer]	[PC]	[SM]	[DAG]
Ctrl.	1	1	1	1
S.D. Ctrl $\sigma^{u=1}$	0.09	–	0.12	0.21
SMS1 overexpr.	1.44*	0.96	1.24*	1.35*
S.D. SMS1 overexpr. $\sigma^{u=2.2}$	0.08	–	0.12	0.27

datasets provided in Ding et al. (2008). The authors considered changes of ceramide, PC, SM and DAG levels in response to overexpression and knockdown of both SMS isoforms. SMS was overexpressed in CHO cells (Table 1 in Ding et al., 2008), and silencing was done in macrophages (Table 2 in Ding et al., 2008). Although lipid levels are given in absolute concentrations in our reference datasets, the data were obtained from two different cell systems, and we normalized them to their cell specific control experiments to be able to test hypotheses across cell lines. The relative changes in lipid concentrations in response to SMS1 manipulations that were extracted from these tables are given in Tables 1 and 2.

To see if our mathematical model is in accordance with the considered data, we interpret the measurements as dynamic equilibrium states $\bar{\mathbf{x}}(u)$, functions of the relative enzymatic activity u, in which the concentrations and hence the reaction fluxes are constant, i.e. $f_i(\bar{\mathbf{x}}(u)) = 0$ for all $i = 1, 2, 3$.

3. Results

Here we prove that only model 2 can qualitatively explain the changes of steady state lipid concentrations taking part in reaction (1) in response to altered SMS1 activities. Furthermore, we show that predictions of the model are in accordance with some other biological results from Villani et al. (2008).

3.1. Model 1 fails to show the qualitative changes in lipid composition in response to SMS1 manipulations

It is expected that changes in the activity of SMS1 impact the net flux of the reversible reaction and thus the dynamic steady state concentrations of the lipids that take part in this reaction. From Tables 1 and 2 it can be seen that the levels of DAG and SM significantly increase or decrease in case of SMS1 overexpression ($u = 2.2$) and silencing ($u = 0.77$), respectively, suggesting that increased SMS1 activity also increases the net flux to the right. Assuming this is true, it is obvious that in model 1 the ceramide level decreases in case of SMS1 overexpression and increases when SMS1 is silenced. However, the values in Tables 1 and 2 show that this is not the case. The observed qualitative changes in lipid concentrations compared to the expected changes are listed in Table 3. In particular, in both experiments ceramide behaves differently than expected regarding model 1: Ceramide levels significantly increase after overexpression of SMS1, and do not change significantly upon silencing of SMS1.

In fact, it can mathematically be shown that the direction of change of the ceramide steady state level after increasing or decreasing the enzymatic activity of SMS1 is always opposite to that of the other two reactants, DAG and SM. For this we assume that the vector field of model (2) is continuously differentiable w.r.t. x and u and the Jacobian matrix $\mathcal{J}_f(\bar{x})$ is invertible. Then, according to the Implicit Function Theorem there exist neighborhoods $U(u_0) \subseteq \mathbb{R}_+$

and $V(\overline{\mathbf{x}}(u_0) := \overline{\mathbf{x}}_0) \subseteq \mathbb{R}^3_+$ and a unique and smooth function $\overline{\mathbf{x}} : U \to V : u \mapsto \overline{\mathbf{x}}(u)$, that represents the steady state of the system as continuous function of u. For this reason we can consider the partial derivative of every variable at steady state $\overline{x}_i(u)$ w.r.t. the imput u. Considering model (2) at steady state we obtain:

$$\begin{aligned} 0 &= C_{in} - d_1 \cdot \overline{x}_1(u) - v(u, \overline{\mathbf{x}}(u), [\mathrm{PC}]) \\ 0 &= -d_2 \cdot \overline{x}_2(u) + v(u, \overline{\mathbf{x}}(u), [\mathrm{PC}]) \\ 0 &= -d_3 \cdot \overline{x}_3(u) + v(u, \overline{\mathbf{x}}(u), [\mathrm{PC}]). \end{aligned} \tag{4}$$

Due to mass conservation the term $v(u, \mathbf{x}, [\mathrm{PC}])$ is the same for all three equations, independent of the exact kinetics. Thus we obtain the following equalities:

$$C_{in} - d_1 \cdot \overline{x}_1(u) = d_2 \cdot \overline{x}_2(u) = d_3 \cdot \overline{x}_3(u). \tag{5}$$

Considering the first equality in Eq. (5) we obtain:

$$\overline{x}_1(u) = \frac{1}{d_1} \cdot (C_{in} - d_2 \cdot \overline{x}_2(u)), \tag{6}$$

and thus if we derive with respect to u:

$$\frac{d\overline{x}_1(u)}{du} = -\frac{d_2}{d_1} \cdot \frac{d\overline{x}_2(u)}{du}, \tag{7}$$

which implies that the direction of change of $\overline{x}_1(u)$ with varying input u is opposite to the direction of change of $\overline{x}_2(u)$.

Using the second equality of Eq. (5) to solve for $\overline{x}_3(u)$,

$$\overline{x}_3(u) = \frac{d_2}{d_3} \overline{x}_2(u), \tag{8}$$

and deriving as well with respect to u leads to

$$\frac{d\overline{x}_3(u)}{du} = \frac{d_2}{d_3} \cdot \frac{d\overline{x}_2(u)}{du}, . \tag{9}$$

which means that the changes of SM and DAG with varying input u are always in the same direction.

Summarizing, model 1 can never lead to a qualitative fit of the data.

3.2. Model 2 shows that the inclusion of a feedback regulation from DAG to ceramide is sufficient to describe experimental data qualitatively

In the following we will show that model 2 which includes the feedback term $C_{in} = f(\mathrm{DAG})$ is able to reproduce the data qualitatively. A comparison of our model output with the available measurements (Table 3) shows that this feedback regulation $C_{in}(x_2)$ must be monotonically increasing, i.e. the overall effect of DAG on the transport rate C_{in} must be positive: First of all, it is obvious that the ceramide steady state level increases monotonically with C_{in}. In case of SMS1 overexpression, DAG also increases. This indicates that SMS1 overexpression increases the flux to the right, which means that more ceramide is converted to SM in this case. Thus, from the original model without feedback we expect that in consequence the ceramide steady state level decreases. We observe, however, that the converse is true, and thus we conclude that an increased DAG level must also increase C_{in} compared to the control experiments. Similarly, DAG decreases in response to SMS1 silencing, since the flux of the reversible reaction to the right decreases, and less ceramide is consumed. Consequently, we expect from the original model that the ceramide steady state level increases compared to the control. However, we observe a slight decrease, although not marked as significant in Ding et al. (2008). This indicates that C_{in} must be reduced in case of SMS1 silencing compared to the control, which is in the case of a positive regulation of DAG onto C_{in} in accordance with the experimentally observed values.

Following the previous calculations (Eqs. (5), (6), (7), (8) and (9)) with $C_{in} = C_{in}(x_2)$, we end up with the following steady state relations:

$$\frac{d\overline{x}_1(u)}{du} = \frac{1}{d_1} \cdot \left(\frac{\partial C_{in}(\overline{x}_2(u))}{\partial x_2} - d_2 \right) \cdot \frac{d\overline{x}_2(u)}{du} \tag{10}$$

$$\frac{d\overline{x}_3(u)}{du} = \frac{d_2}{d_3} \cdot \frac{d\overline{x}_2(u)}{du}. \tag{11}$$

The second equation states again that DAG and SM change in the same direction with varying input u. Furthermore, it is easy to see that if

$$\frac{\partial C_{in}(\overline{x}_2(u))}{\partial x_2} > d_2, \quad \forall \overline{x}_2(u), \tag{12}$$

is fulfilled, i.e. in case of increasing u the loss of ceramide due to the increased flux of the reversible reaction is overcompensated by the gain from the positive feedback loop in the system, then the changes of the steady states for varying input u have the same direction for all variables $\overline{x}_1(u), \overline{x}_2(u)$ and $\overline{x}_3(u)$. We conclude that model 2 is able to represent experimental findings qualitatively.

Table 2
Lipid concentrations and respective standard deviations in SMS1 knockdown THP-1-derived macrophages, which resulted in a 23% decrease in SMS1 activity. Values according to Table 2 in Ding et al. (2008) and normalized to the levels in the control experiments. Values labeled with an asterisk were marked as statistically significant changes compared to the control in the original publication.

Type of experiment	[Cer]	[PC]	[SM]	[DAG]
Ctrl.	1	1	1	1
S.D. Ctrl $\sigma^{u=1}$	0.08	–	0.11	0.05
SMS1 knockdown	0.95	1.06	0.8*	0.76*
S.D. SMS1 knockdown $\sigma^{u=0.77}$	0.12	–	0.09	0.10

Table 4
Summary of the findings of Villani et al. (2008) compared with our model predictions. Their conclusions show a qualitative agreement with our model predictions.

Exp. no.	Source	Manipulation	Golgi PKD	Expected model response	Agreement
1	Fig. 12 A–C	SMS1 ↓	↓	C_{in} ↓ Fig. 2	✓
2	Fig. 11 E–G	Ceramide ↑	↑	C_{in} ↑ Fig. 2	✓

Table 3
Comparison between experimental observations and expected response of model 1. Shown are the qualitative changes in dynamic lipid steady state concentrations after SMS1 manipulations.

Comparison	$\overline{[\mathrm{Cer}]}$		$\overline{[\mathrm{PC}]}$		$\overline{[\mathrm{DAG}]}$		$\overline{[\mathrm{SM}]}$	
Manipulation	SMS1 ↑	SMS1 ↓	SMS1 ↑	SMS1 ↓	SMS1 ↑	SMS1 ↓	SMS1 ↑	SMS1 ↓
Data	↑	–	–	–	↑	↓	↑	↓
Expected	↓	↑	–	–	↑	↓	↑	↓

3.3. Experimental SM synthesis manipulation changes PKD Golgi localization and supports the proposed feedback mechanism

In this subsection we show that the proposed feedback mechanism of model 2 agrees with both CHO and macrophage data from Ding et al. (2008) and experiments with HeLa cells by Villani et al. (2008). Villani showed that treatment of HeLa cells with SMS1 siRNA and C_6-ceramide results in lower and higher PKD Golgi localization, respectively. Their qualitative findings are summarized in Table 4 columns 1–4.

Following the feedback hypothesis of Fig. 1, PKD localization is an indicator for our proposed model feedback term C_{in} and should qualitatively show the same up and downward regulation behavior as the feedback itself: PKD $\propto C_{in}$, and, since $C_{in}(x_2)$ is monotonically increasing, also PKD $\propto \overline{x}_2$. We have already seen that a lower SMS1 stimulus causes a decrease in $\overline{x}_2$, which is thus in agreement with those data.

In the second experiment, the upward shift of the steady state feedback term $C_{in}(\overline{x}_2(u))$ can, to our knowledge, not easily be shown analytically. A second artificial inflow of ceramide, $C_{\exp}$, needs to represent treatment with C_6-ceramide in the first differential equation of model 2 to account for the correct experimental condition:

$$\dot{x}_1 = C_{in}(x_2) - d_1 x_1 - v(u, \mathbf{x}, [\mathrm{PC}]) + C_{\exp}. \tag{13}$$

We would have to show that adding $C_{\exp}$ increases $C_{in}(\overline{x}_2)$ or $\overline{x}_2$, which is equivalent. However, the change in $\overline{x}_2$ depends on that of $\overline{x}_1$ and on the flux $v(\overline{x}, u)$, and the result is not independent of the flux any more.

Thus, in order to compare our results with this second experiment, we used Bayesian inference to train our model to the dataset of Ding et al.. Subsequently, we simulated the predictions for the experiments of Villani et al. with the calibrated model. For this purpose we employed the simple case of a linear feedback term $C_{in}(x_2) = a x_2$, and used the following two fluxes for the reversible reaction (1), where the net flux considered in model (2) is simply given by $v(u, \mathbf{x}, [\mathrm{PC}], p_1, k_1) = v_1(u, x_1, [\mathrm{PC}], p_1, k_1) - v_2(u, x_2, x_3, p_2, k_2)$:

$$v_1(u, x_1, [\mathrm{PC}], p_1, k_1) = p_1 u \frac{x_1[\mathrm{PC}]}{x_1[\mathrm{PC}] + k_1} \tag{14a}$$

$$v_2(u, x_2, x_3, p_2, k_2) = p_2 u \frac{x_2 x_3}{x_2 x_3 + k_2}. \tag{14b}$$

These are simpler than the substituted-enzyme-kinetics proposed for this reaction (Cornish-Bowden, 2004), in particular contain less parameters, which is advantageous for parameter estimation, but can still account for saturation in case of limited enzyme. As Bayesian inference returns a parameter sample from a parameter distribution describing the agreement with a dataset, predictions based on this method also come in the form of predictive distributions as in Fig. 2. The dashed curve in Fig. 2 depicts the distribution of feedback response relative to the control after SMS1 silencing $p(C_{in}^{exp1,2}/C_{in}^{control}|\mathcal{D})$ conditioned on the Ding et al. dataset $\mathcal{D}$. The solid curve depicts the distribution after addition of external ceramide. All values of the two distributions are below or above the control value of 1 respectively, and are thus in agreement with the data in Table 4.

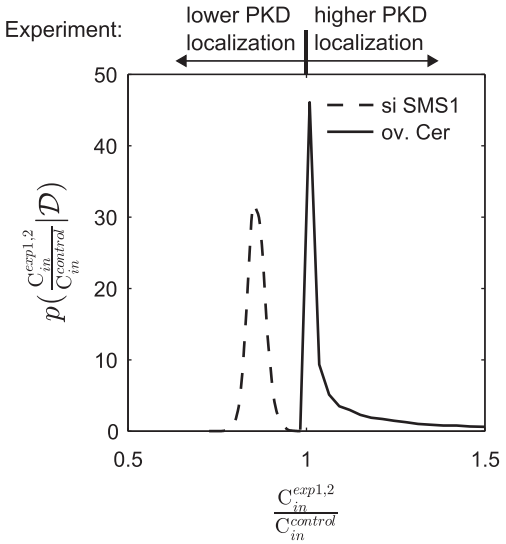

Fig. 2. Predicted distribution of the normalized steady state model feedback term $C_{in}^{exp\ 1,2}/C_{in}^{control}$ when simulating the experiments: ceramide overexpression and SMS1 silencing, respectively. An amplification and damping of the feedback relative to the control (x-axis value 1) is observed.

4. Discussion

We have introduced a model based on chemical reaction kinetics to describe the SMS1 driven reversible conversion of ceramide and phosphatidylcholine to sphingomyelin and diacylglycerol. We showed that a simple model that considers this reversible reaction in isolation is not able to capture the experimental findings, in particular, changes of ceramide levels in response to SMS1 overexpression and silencing could not be explained by the model. Based on these findings, and on biological knowledge, we modified the model by including a positive feedback regulation from DAG on the right-hand side of the reaction onto ceramide on the left-hand side. We proved that in the modified model a set of feedback functions, including e.g. linear feedback, is able to explain the data. Finally we supported our proposed feedback idea via PKD by comparing predictions of the model with experimental findings from literature of PKD enrichment at the TGN under different experimental conditions.

Our results indicate that feedback regulation might be important for the SMS1 driven conversion of ceramide to sphingomyelin, and that such feedback can cause effects *in vivo* that cannot be explained by regarding the SMS1 driven conversion in isolation *in silico*. Although we have motivated the existence of such a feedback here with an indirect influence of DAG to the efficiency of ceramide transport to the trans-Golgi network involving protein kinase D and the ceramide transfer protein CERT, we do not know whether this pathway has the main contribution to this feedback effect, and there might be other explanations as well.

In fact, the overall effect on ceramide due to modulation of SMSs is not yet fully understood in detail. While the data of Villani et al. (2008) supports a feedback via PKD, this might be differently regulated depending on the specific cellular context. In resting Jurkat and CHO cells, for example, overexpression of SMS1 and SMS2 caused an increase of ceramide as part of a general stimulation of sphingolipid synthesis, whereas in Jurkat cells it prevented accumulation of ceramide in response to photodamage (Subathra et al., 2011, and references therein).

Although positive feedback is a possible explanation for the data, we do not claim that the feedback must be positive under all conditions. Gupta et al. (2011) observed a positive effect on ceramide levels when simultaneously lifting cellular DAG and PC levels to train their lipid metabolism model. Since they did a rather cell global perturbation, in contrast to a TGN specific manipulation, they incorporated a different positive feedback in their model to explain such effects: an edge from SM to ceramide over PM and lysosome related Acid SMase reactions.

One critical point we see in this study is the difference between changes in global and local lipid pools. Here we considered a reaction that takes part mainly at the trans Golgi network,

but might also have an effect on lipid composition in other parts of the cell. Furthermore, unfortunately we only have whole cell data available. Since these data only provide limited information about the dynamics of the system under study, the models are kept as simple as possible in order to reduce the number of free parameters. Among others, for example, we have to make the assumption that the experimental changes seen globally also reflect the local changes.

Moreover, the results must also be reflected in the context of further metabolic pathways of ceramide adjoining the model boundaries. These pathways are simplified here via constant inflow or linear degradation terms. In mammalian cells the de novo synthesis of ceramide starts with palmitoyl CoA and L-serin. In four enzyme catalyzed reactions ceramide is synthesized in the cytoplasmic leaflet of the ER membrane. It is known that the bulk of this newly synthesized ceramide is transported to the trans-Golgi by the ceramide transfer protein CERT (Hanada, 2010). At the TGN, the major amount is converted via the modeled SMS1 reaction to sphingomyelin. A smaller amount is converted to ceramide-1-phosphate via ceramide kinase (Hussain et al., 2012). Since CERT manipulation did not effect glucosylceramide (GlcCer) production at the Golgi, it was suggested that the ceramide pool for this reaction is dependent on a different transport mechanism (Hanada et al., 2003). Due to the fact that we are observing cell global pools, the model's linear ceramide degradation term summarizes and thereby approximates all these remaining outflows. Due to the sparse data situation more complex responses from other pathways such as perturbations of ER related sphingosine or PM induced sphingosine-1-phosphate production from ceramide (Hannun and Obeid, 2008) are not addressed in this study.

DAG is likely one of the most connected lipids and its metabolism is very complex (Carrasco and Mérida, 2007). Therefore multiple connected DAG pathways also serve as a rich basis for model extensions. Two possible TGN related inflows beside SMS1 triggered conversion are possible: a) phospholipase D (PLD) converts PC into phosphatidic acid (PA), which is dephosphorylated by PA phosphohydrolases (PAP) or lipid phosphate phosphatases (LPP), thus generating DAG (Lev, 2010; Bard and Malhotra, 2006); b) PI(4)P or PI(4,5)P2 is converted into DAG via some specific phospholipase C (PLC) (Bard and Malhotra, 2006). If we consider degradation, DAG acts as a precursor of phosphatidylethanolamine and phosphatidylcholine (PC), catalyzed by choline/ethanolamine phosphotransferase (CEPT1) located in the ER and in the external nuclear membrane and by choline phosphotransferase (CPT), located at the Golgi (Carrasco and Mérida, 2007). This last pathway, also known as CDP-choline pathway, is highly controlled by the Nir2 Golgi protein, whose role is to keep a critical DAG pool in the Golgi apparatus, which is essential for maintaining the structural and functional integrity of the Golgi apparatus in mammalian cells (Litvak et al., 2005; Bard and Malhotra, 2006). This direct relationship between PC and DAG could be reconsidered when extending the model in presence of special data comprising specific PC levels at the TGN.

We are aware that perturbations of the simple subsystem under consideration may cause a response that involves one or more of the discussed connected pathways. If this happens and their influence becomes dominating, the overall behavior may not be satisfactorily explained by the simple model under study. Therefor, only context based monitoring of available data and continuous expansion of the SMS network will lead to its holistic understanding.

Contributions

Caterina Thomaseth, Patrick Weber and Nicole Radde elaborated the model, the numerical and theoretical results and wrote the article. Thomas Hamm supported with the biological foundation of the article. Kenji Kashima elaborated preliminary models and theoretical results. All authors have read and approved the final manuscript.

Funding

PWe and NR acknowledge financial support from the German Research Foundation (DFG) (GZ:RA 1840/1-1), and from the German Research Foundation within the Cluster of Excellence in Simulation Technology (EXC 310/1) at the University of Stuttgart. CT acknowledges funding by the Federal Ministry of Education and Research (BMBF) via the project PREDICT (FKZ 0316186A).

Acknowledgments

The authors want to thank Dr. Angelika Hausser and Prof. Monilola Olayioye from the Institute of Cell Biology and Immunology Stuttgart, for support in biological questions and the proof reading of the manuscript. We additionally thank Eva-Maria Geissen from the Institute for Systems Theory and Automatic Control in Stuttgart for proof reading and support. We also want to thank the referees, who did an excellent job in improving the manuscript.

Appendix A. Sampling-based parameter estimation and model predictions

For a general introduction to Bayesian model and data analysis we refer to Gelman et al. (2004) and Wilkinson (2006). All basic numerical calculus has been performed using `MATLAB R2011b` (64 bit). For model and data management the `SBtoolbox2` (Schmidt and Jirstrand, 2006) has been used. For numerical integration of the ODE systems `SBtoolbox2` built in CVODE integrators from the `SUNDIALS` suite has been employed (Cohen and Hindmarsh, 1996) (http://www.llnl.gov/CASC/sundials/). Absolute and relative error tolerances of the integrator has been set to at least `option.abstol=1e-6` and `option.reltol=1e-6`. To avoid stiffness problems the number of maximal steps for the second model has been increased to `options.maxnumsteps=1e6`.

In the study maximum likelihood estimates (MLE) of parameters have been utilized to look for example at a first model fit and to determine the prior support region. A log-normal error model has been employed to the data using the standard deviations given in the main article in Tables 1 and 2. To guarantee reliable maximum likelihood estimates a multiple start optimization algorithm using the Matlab `fmincon` solver with an absolute and relative tolerance of `OPTIONSfmincon.TolFun=1e-6` and `OPTIONSfmincon.TolCon=1e-6` has been employed.

For the Markov chain Monte Carlo (MCMC) sampling the Matlab based objective function is anonymously passed on to the `mcmcstat` sampling toolbox (Haario et al., 2006). Sampling is performed in the logarithmic parameter space with a log uniform bounded prior, spanning over four orders of magnitude. The support region was centered around the maximum likelihood estimate. Two Markov chains are started in parallel. A warm up/tuning of the covariance based proposal distribution is performed by drawing a sample of size 10^4 using the 'DRAM' sampling method from the `mcmcstat` toolbox. For the model with linear feedback, two chains with a sample size of 3×10^6 are generated. Convergence has been tested with the `mcmcstat` built-in Geweke method (Brooks and Roberts, 1998). All chains passed the convergence test with a p-value of at least 0.8 in each sub-dimension. The resulting merged chains 6 million sampled points respectively

with p-values of 0.8 or higher in each sub-dimension. The acceptance rate was about 32%.

An overview of the numerical Bayesian analysis:

1. Initialize model and the data.
2. Run a parallel multi-start optimization to gain initial MLE fit with Ding et al. data.
3. Determine boundaries of initial uniform prior centered two orders of magnitude around the MLE.
4. Run a warm up sampling with two parallel Markov chains. Run a two chain sampling main run.
5. Chain merging and convergence analysis.
6. Computation of posterior predictive distributions for the Villani et al. experiments.

To account for the experimental conditions in the ceramide treatment experiment of Villani et al., the magnitude of the additional C_{exp} was chosen to be ten fold higher then the mean control experiment inflow $C_{in}^{control}$. A representative subsample of 1×10^3 parameters is taken from the parameter posterior distribution to calculate the prediction distributions in Fig. 2. Further details and MATLAB code can be provided by the authors upon request.

References

Bard, F., Malhotra, V., 2006. The formation of TGN-to-plasma-membrane transport carriers. Annual Review of Cell and Developmental Biology 22, 439–455.

Brooks, S.P., Roberts, G.O., 1998. Assessing convergence of Markov chain Monte Carlo algorithms. Statistics and Computing 8, 319–335.

Carrasco, S., Mérida, I., 2007. Diacylglycerol, when simplicity becomes complex. Trends in Biochemical Sciences 32, 27–36.

Cohen, S., Hindmarsh, C., 1996. Cvode, a stiff/nonstiff ode solver in C. Computers in Physics 10, 138–143.

Cornish-Bowden, A., 2004. Fundamentals of Enzyme Kinetics. Portland Press.

Ding, T., Li, Z., Hailemariam, T., Mukherjee, S., Maxfield, F., Wu, M.-P., Jiang, X.-C., 2008. SMS overexpression and knockdown: impact on cellular sphingomyelin and diagylglycerol metabolism, and cell apoptosis. Journal of Lipid Research 49, 376–385.

Fugmann, T., Hausser, A., Schöffler, P., Schmid, S., Pfizenmaier, K., Olayioye, M., 2007. Regulation of secretory transport by protein kinase D-mediated phosphorylation of the Ceramide Transfer Protein. Journal of Cell Biology 178, 15–22.

Gelman, A., Carlin, J., Stern, H., Rubin, D., 2004. Bayesian Data Analysis, Texts in Statistical Science, 2 edition Chapman & Hall, CRC.

Gupta, S., Maurya, M.R., Merrill Jr., A.H., Glass, C.K., Subramaniam, S., 2011. Integration of lipidomics and transcriptomics data towards a systems biology model of sphingolipid metabolism. BMC Systems Biology 5, 26.

Haario, H., Laine, M., Mira, A., Saksman, E., 2006. DRAM: efficient adaptive MCMC. Statistics and Computing 16, 339–354, http://dx.doi.org/10.1007/s11222-006-9438-0.

Hanada, K., 2010. Intracellular trafficking of ceramide by ceramide transfer protein. Proceedings of the Japan Academy – Series B: Physical & Biological Sciences 86, 426–437.

Hanada, K., Kumagai, K., Yasuda, S., Miura, Y., Kawano, M., Fukasawa, M., Nishijima, M., 2003. Molecular machinery for non-vesicular trafficking of ceramide. Nature 426, 803–809.

Hanada, K., Kumagai, K., Yasuda, S., Miura, Y., Kawano, M., Fukasawa, M., Nishijima, M., 2003. Molecular machinery for non-vesicular trafficking of ceramide. Nature 426, 803–809.

Hannun, Y.A., Obeid, L.M., 2008. Principles of bioactive lipid signalling: lessons from sphingolipids. Nature Reviews Molecular Cell Biology 9, 139–150.

Hausser, A., Storz, P., Märtens, S., Link, G., Toker, A., Pfizenmaier, K., 2005. Protein kinase D regulates vesicular transport by phosphorylating and activating phosphatidylinositol-4 kinase III β at the Golgi complex. Nature Cell Biology 7, 880–886.

Holthuis, J.C.M., Luberto, C., 2010. Tales and mysteries of the enigmatic sphingomyelin synthase family. Advances in Experimental Medicine and Biology 688, 72–85.

Huitema, K., van den Dikkenberg, J., Brouwers, J.F.H.M., Holthuis, J.C.M., 2004. Identification of a family of animal sphingomyelin syntheses. EMBO Journal 23, 33–44.

Hussain, M.M., Jin, W., Jiang, X.-C., 2012. Mechanisms involved in cellular ceramide homeostasis. Nutritition & Metabolism (London) 9, 71.

Kudo, N., Kumagai, K., Tomishige, N., Yamaji, T., Waktsuki, S., Nishijima, M., Hanada, K., Kato, R., 2008. Structural basis for specific lipid recognition by CERT responsible for nonvesicular trafficking of ceramide. Proceedings of the National Academy of Science USA 105, 488–493.

Lev, S., 2010. Non-vesicular lipid transport by lipid-transfer proteins and beyond. Nature Reviews Molecular Cell Biology 11, 739–750.

Litvak, V., Dahan, N., Ramachandran, S., Sabanay, H., Lev, S., 2005. Maintenance of the diacylglycerol level in the Golgi apparatus by the Nir2 protein is critical for Golgi secretory function. Nature Cell Biology 7, 225–234.

Pusapati, G.V., Krndija, D., Armacki, M., von Wichert, G., von Blume, J., Malhotra, V., Adler, G., Seufferlein, T., 2010. Role of the second cysteine-rich domain and Pro275 in protein kinase D2 interaction with ADP-ribosylation factor 1, trans-Golgi network recruitment, and protein transport. Molecular Biology of the Cell 21, 1011–1022.

Sarri, E., Sicart, A., Lázaro-Dieǵuez, F., Egea, G., 2011. Phospholipid synthesis participates in the regulation of diacylglycerol required for membrane trafficking at the Golgi complex. Journal of Biological Chemistry 286, 28632–28643.

Schmidt, H., Jirstrand, M., 2006. Systems biology toolbox for MATLAB: a computational platform for research in systems biology. Bioinformatics 22, 514–515.

Subathra, M., Qureshi, A., Luberto, C., 2011. Sphingomyelin synthases regulate protein trafficking and secretion. PLoS One 9, e23644.

Tafesse, F., Huitema, K., Hermansson, M., van der Poel, S., van den Dikkenberg, J., Uphoff, A., Somerharju, P., Holthuis, J., 2007. Both sphingomyelin synthases SMS1 and SMS2 are required for sphingomyelin homeostasis and growth in human HeLa cells. Journal of Biological Chemistry 282, 17537–17547.

Villani, M., Subathra, M., Im, Y.-B., Choi, Y., Signorelli, P., del Poeta, M., Luberto, C., 2008. Sphingomyelin synthases regulate production of diacylglycerol at the Golgi. Biochemical Journal 414, 31–41.

van Meer, G., Voelker, D.R., Feigenson, G.W., 2008. Membrane lipids: where they are and how they behave. Nature Reviews Molecular Cell Biology 9, 112–124.

Wilkinson, D., 2006. Stochastic Modelling for Systems Biology, Mathematical and Computational Biology, volume 11. Chapman & Hall/CRC.